Fermi National Accelerator Laboratory

FERMILAB-Pub-93/261-A
August, 1993

Production of Li, Be & B from Baryon Inhomogeneous Primordial Nucleosynthesis *

David Thomas[1], David N. Schramm[1,2], Keith A. Olive[3],
Grant J. Mathews[4], Bradley S. Meyer[5], Brian D. Fields[1]

[1] University of Chicago, Chicago, IL 60637
[2] NASA/Fermilab Astrophysics Center, FNAL, Box 500 Batavia, IL 60510
[3] University of Minnesota, School of Physics and Astronomy, Minneapolis, MN 55455
[4] Lawrence Livermore National Laboratory, Livermore, CA 94550
[5] Department of Physics and Astronomy, Clemson University, Clemson, SC 29634-1911

Abstract

We investigate the possibility that inhomogeneous nucleosynthesis may eventually be used to explain the abundances of ^{6}Li, ^{9}Be and B in population II stars. The present work differs from previous studies in that we have used a more extensive reaction network. It is demonstrated that in the simplest scenario the abundances of the light elements with $A \leq 7$ constrain the separation of inhomogeneities to sufficiently small scales that the model is indistinguishable from homogeneous nucleosynthesis and that the abundances of ^{6}Li, ^{9}Be and B are then below observations by several orders of magnitude. This conclusion does not depend on the ^{7}Li constraint. We also examine alternative scenarios which involve a post-nucleosynthesis reprocessing of the light elements to reproduce the observed abundances of Li and B, while allowing for a somewhat higher baryon density (still well below the cosmological critical density). Future B/H measurements may be able to exclude even this exotic scenario and further restrict primordial nucleosynthesis to approach the homogeneous model conclusions.

* submitted to *The Astrophysical Journal*

1. Introduction

There has been considerable recent interest in the possibility that baryons may have been distributed inhomogeneously in the early universe. There are a number of mechanisms by which such inhomogeneities could be produced (c.f. Malaney & Mathews, 1993). Perhaps the most frequently considered has been a first-order QCD phase transition. It is quite possible that density inhomogeneities could be produced (Crawford and Schramm 1982; Hogan 1983; Witten 1984; Iso, Kodama & Sato 1986; Fuller, Mathews & Alcock 1988; Kurki-Suonio 1988; Kapusta and Olive 1988). These perturbations may have had a profound effect on the production of the light elements in the early universe (Applegate and Hogan 1985; Sale and Mathews 1986; Applegate, Hogan & Scherrer 1987; Alcock, Fuller & Mathews 1987; Malaney and Fowler 1988; Kurki-Suonio and Matzner 1989 and 1990; Terasawa and Sato 1989a,b,c; Kurki-Suonio, Matzner, Olive & Schramm 1990; Mathews, Meyer, Alcock & Fuller 1990). In this paper we examine the consequences of inhomogeneous nucleosynthesis on the intermeditate stable isotopes ^{6}Li, ^{9}Be, ^{10}B and ^{11}B.

In recent years measurements have been made in population II stars of elements that were once thought to have been produced in insignificant quantities in the standard homogeneous big bang. One of these, ^{9}Be (Rebolo et al. 1988; Ryan et al. 1992; Gilmore, Edvardsson, & Nissen 1991) has been proposed (Boyd, & Kajino 1989; Malaney, & Fowler 1989) as a potential signature of baryon-inhomogeneous nucleosynthesis. However the strong observed correlation of Be/H with metallicity implies that it was made in the early Galaxy (Walker et al. 1993, Fields, Schramm & Truran 1993). To date, population II B/H data includes only three measurements (Duncan, Lambert, & Lemke 1992), which again show a correlation with metallicity. There has been one observation so far of ^{6}Li (Smith, Lambert, & Nissen 1992).

These data appear to be best explained by galactic cosmic ray spallation (Steigman & Walker 1992; Walker et al. 1993; Prantzos, Cassé, & Vangioni-Flam 1993; Olive and Schramm 1992; Steigman et al. 1993), however there remains the question of whether

^{6}Li, Be and B can be produced by primordial nucleosynthesis, and if so whether they can provide the much sought after litmus test of baryon inhomogeneities in the early universe. Four of us (Thomas et al. 1993, hereafter TSOF) used the largest network to date (in terms of reactions influencing light, $A \leq 12$, element abundances) to demonstrate that standard homogeneous big bang nucleosynthesis underproduces these nuclei by at least 2 (^{6}Li), 4 (^{9}Be) and 5 (B) orders of magnitude, when the abundances of the lighter elements and ^{7}Li are compared to the observations. In this paper we investigate inhomogeneous yields using an even further extension of the reaction network developed in TSOF. Our work primarily differs from previous similar studies (e.g. Terasawa & Sato, 1989c) in that we have considered a larger network of reactions to produce ^{6}Li, ^{9}Be, ^{10}B and ^{11}B, fully allowing for neutron-rich flows and multiple back-reactions.

Nucleosynthesis in a homogeneous big bang requires the evolution of a set of equations representing the rates of the nuclear reactions in the network. The only input parameter is the baryon to photon ratio $\eta = n_B/n_\gamma$ or equivalently the density of baryons, (since n_γ can be directly related to the microwave background temperature). Additional parameters are introduced when the effects of baryon inhomogeneities are taken into account. One of these parameters is the length scale, l, associated with the fluctuations. If this length scale is much greater than the neutron diffusion length then diffusion is unimportant and the yields can be obtained by simply averaging the yields from regions with different baryon densities (Wagoner, 1973; Yang et al. 1984). In the homogeneous model however, data on D and He restrict the baryon density to a small range about $\eta_{10} = 3$ ($\eta_{10} = \eta/10^{-10}$) where ^{7}Li takes on its minimum value (^{7}Li/H $\sim 10^{-10}$) in agreement with observations (Spite & Spite 1982a,b,1986; Hobbs and Duncan 1987; Rebolo, Molaro & Beckman 1988). Any average of the $\eta_{10} = 3$ solution with that for another value of η will increase the ^{7}Li abundance, and is likely to violate the upper limit (1.4×10^{-10}). Thus one obtains strong constraints on the amplitude of such perturbations.

In the other extreme (inhomogeneities much smaller than the neutron diffusion length) baryon diffusion will eradicate the inhomogeneities before nucleosynthesis begins, and we return to the homogeneous case. It is the intermediate case that interests us here. When the inhomogeneity scale is of the same order as the neutron diffusion length the more rapid diffusion of neutrons (compared to protons) leads to an inhomogeneity in n/p in addition to the density inhomogeneity. The earliest studies of this scenario (Applegate, Hogan & Scherrer 1987; Alcock et al. 1987) assumed that neutrons diffused to a homogeneous density before nucleosynthesis began, and neglected all diffusion effects during nucleosynthesis. This simple model was able to satisfy constraints from ^{2}H and ^{4}He (and ^{3}He) with a baryon density equal to the critical value ($\Omega_B = 1$) and a density contrast (~ 100) that seemed not implausible from the point of view of quark-hadron physics. This scenario was attractive because it did away with the need for non-baryonic dark matter. Unfortunately, it overproduced ^{7}Li. It was later suggested that the excess Li may be removed by diffusion of neutrons back into the high density region after nucleosynthesis (Malaney and Fowler 1988) for values of $l \sim 10$ m. Though this turns out to be only partially true (Terasawa & Sato, 1989; Kurki-Suonio & Matzner, 1989; Mathews et al., 1990), the important lesson is that an accurate determination of abundances requires a calculation which takes careful account of the diffusion of neutrons and protons before, during and after nucleosynthesis.

In recent years, more detailed diffusion calculations (Kurki-Suonio and Matzner 1989 and 1990; Terasawa and Sato 1989a,b,c; Mathews, Meyer, Alcock & Fuller 1990; Kurki-Suonio, Matzner, Olive, & Schramm, 1990) have shown that not only could ^{7}Li be affected but ^{4}He as well. It was found that nucleosynthesis with $\Omega_B = 1$, no matter what the density contrast, overproduced both ^{4}He and ^{7}Li.† Indeed these latest calculations all showed that for $\Omega_B = 1$, and when the distance scale of the inhomogeneities, l is greater than 30 m only the D abundance can be brought into agreement with observations. Though the standard

† The problem with ^{4}He is particularly important since it does not allow for the possibility that consistency of all the light elements is achievable simply by the depletion of ^{7}Li in non-standard solar models

model constraints on η can be modified, the modification was shown to be rather limited (Kurki-Suonio, Matzner, Olive & Schramm 1990).

In this paper we have used the diffusion code developed by Mathews et al. (1990). Initial density fluctuations are arranged in a lattice of spheres with separation $l = 2r$. Each sphere is described as a high density core and a low density outer shell. The core has density and radius of R and $f_v^{1/3}$ respectively, relative to the outer region. The sphere is divided up into concentric spherical zones, with a higher resolution near the boundary between high and low density regions. We expect the choice of spherical boundary conditions to maximize the potential effect. In all results presented here we have used 16 concentric zones. We have also run test cases with 8 and with 32 zones, indicating that 16 provide adequate accuracy, while remaining economical with computer time (Mathews et al. 1990). We also note that results of this code are consistent with those of Terasawa and Sato (1989a–c) and Kurki-Suonio and Matzner (1989).

To alleviate some of the problems encountered in inhomogeneous models, mechanisms have been proposed to reprocess the nucleosynthesis products subsequent to the epoch of primordial nucleosynthesis. These mechanisms in particular reduce the abundance of ^{7}Li, thus (potentially) allowing for higher Ω_B models. One such mechanism (Alcock et al., 1990; Jedamzik, Fuller & Mathews, 1993a) examines a fluid mechanical property of the electromagnetic plasma near the end of nucleosynthesis. The photon mean free path λ_γ and the average physical (i.e. not comoving) size l_h of the high density regions have different temperature dependences. At high temperatures ($T \gtrsim 20$ keV), $\lambda_\gamma < l_h$, and so the EM plasma is confined over regions smaller than the baryon fluctuations, thus preserving these fluctuations. Below $T = T_m \sim 20$ keV, however, $\lambda_\gamma > l_h$, and the EM plasma is not confined on the fluctuation scales. Protons in the high density regions flow out, hindered only by radiation (Thomson) drag. Alcock et al. (1990) argue that the dissipation of the fluctuations will homogenize the universe. They model this effect by running the inhomogeneous code to a given T_m, then following the rest of the evolution in the standard (homogeneous) code. They find that for the favored range of T_m there is a significant reduction in the final abundances of Li, Be, and B over inhomogeneous production without dissipation, with ^{7}Li/H in particular reduced from $\sim 10^{-9}$ to $\sim 10^{-10}$. However, detailed calculations of Jedamzik et al. (1993) have shown that this mechanism is not as efficient as was previously believed.

Gnedin and Ostriker (1993) have suggested another model of reprocessing, in which a baryon rich universe ($\Omega_B^0 \simeq 0.15$) overproduces ^{4}He and ^{7}Li, while underproducing ^{2}H and ^{3}He. They then posit that Jeans-mass black holes are formed at recombination. The black holes form accretion disks which emit a photon flux and reprocesses the ambient material; in particular, photodissociating the light elements and producing ^{2}H and ^{3}He by dissociating ^{4}He. The net effect could be to reproduce the observed levels of ^{2}H and ^{3}He, while still overproducing ^{7}Li by a factor of 10, and producing ^{4}He at a level of $Y_p \simeq 0.250$.

We will discuss the implications of reprocessing on our conclusions.

2. The calculation

Based on the reaction network developed earlier (TSOF) and extended where necessary to allow for neutron-rich flows etc., we have evaluated the yields of the light elements from inhomogeneous primordial nucleosynthesis. The earlier reaction network contained 180 reactions, see table 1 of TSOF. However, as pointed out in TSOF, the "flow" to the heavier elements (Be, B) lies largely along the neutron-rich side of the network, and thus mainly occurs in the low density, neutron rich zones of the inhomogeneous model. We felt it wise therefore to update the network further. The 84 additional reaction rates were estimated using the methods outlined in TSOF and Fowler and Hoyle (1964), and are shown in table 1. The full network is shown in figure 1. We have run a few sample cases without the extra reactions, and find no significant effect on the results.

The diffusion code of Mathews et al. (1990) includes full multi-zoning and neutron back-diffusion. The diffusion coefficients used were those calculated by Banerjee & Chitre

(1991), and Kurki-Suonio et al. (1992). Results were obtained for a wide range of values for η and r with the density contrast fixed at $R = 10^2, 10^3$, and fractional volumes (for the high density region) $f_v = 1/64, 1/8$. We have also calculated results for $R = 10^6$ with $f_v = 1/64$. The geometry assumed was spherical, with 16 concentric zones and a high density core. Due to the small uncertainty in the neutron mean life ($\pm$ 2.1 sec) we fix this value at 889.1 s. (Particle Data Group, 1992).

Baryon inhomogeneities have been best motivated by a possibility of a first-order QCD phase transition. Though the values of R and r can not yet be reliably predicted by QCD, some estimates can be made. For example, if chemical equilibrium is maintained, the value of R, which is very sensitive to the transition temperature T_c,is found to be between $7 < R < 100$ for $T > 100$ MeV (Alcock et al., 1987; Kapusta & Olive, 1988). More generally, the value of R is determined by a combination of the enhanced thermodynamic solubility of baryon number in the high-temperature phase and the limited baryon number permeability of the moving phase boundary. Depending on the efficiency of baryon transport and the baryon penetrability of the phase boundary; R may be considerably larger (Witten, 1984; Fuller et al., 1988; Kurki-Suonio, 1988). The ultimate value at the time of nucleosynthesis, however, is expected to be less than 10^6 due to the effects of neutrino-induced heating and expansion of the fluctuations (Heckler & Hogan, 1993; Jedamzik et al., 1993a,b). The baryon number build-up at the boundary surface (where R is largest) contains only a small fraction of the total baryon number (Kurki-Suonio 1988). Thus, though we include values of R as large as 10^6 in our calculations, this should be viewed as an extreme upper limit.

The value of r is also very sensitive to T_c and the surface tension, σ, of the phase interface (Fuller, Mathews & Alcock 1988; Kajantie, Karkkainen & Rummukainen 1990); $r \simeq 2 \times 10^4 m (\frac{\sigma}{MeV^3})^{3/2} (\frac{T_c}{MeV})^{-13/2}$. For values of $\sigma^{1/3} \simeq 70$ MeV estimated by Fahri and Jaffe (1984) which agree with the effective field theory model estimates (Campbell, Ellis & Olive 1990), $r \lesssim 0.4m$ for $T_c \gtrsim 100$ MeV. This is to be compared with preferred values of $r \approx 30$ m or the more recent estimates (Kurki-Suonio et al. 1992) of $r \approx 100$ m at which reductions (though still insufficient) in the production of ^{4}He and ^{7}Li occur. It is important to note that the available estimates from QCD are all perfectly compatible with *homogeneous* nucleosynthesis.

3. Results

Results are shown in figures 2–8. Figure 2a shows the η–r plane (where η is the baryon to photon ratio, n_B/n_γ and r is the radius of the spherical regions in cm, measured at 100 MeV, after the phase transition) for $R = 100$ (results for $f_v = 1/8$ and $f_v = 1/64$ are combined). The contours show observational limits on the abundances of the light elements (Walker et al. 1991 (WSSOK) and refs. therein):

$$0.22 \le Y_p \le 0.24 \tag{1}$$

$$^2\mathrm{H/H} \ge 1.8 \times 10^{-5} \tag{2}$$

$$(^2\mathrm{H} + ^3\mathrm{He})/\mathrm{H} \le 1.0 \times 10^{-4} \tag{3}$$

$$1.0 \times 10^{-10} \le ^7\mathrm{Li/H} \le 1.4 \times 10^{-10}. \tag{4}$$

In addition, the dashed curve represents a He mass fraction $Y_p = 0.245$ which is the most recently derived (preliminary) upper limit on Y_p (Skillman et al. 1993). The region which satisfies all these constraints is hatched. Note that the only effect of increasing the maximum He abundance to 0.245 is to allow a slightly higher value of r. Figure 2b shows similar data for $R = 1000$, and 2c for $R = 10^6$. Note that in figures 2 the hatched regions cover a similar area.

For small r ($\lesssim 100$ cm), diffusion eliminates inhomogeneities before nucleosynthesis begins and the results are identical to those from a homogeneous calculation. As r increases from 100 cm, the He mass fraction rises rapidly above 0.24. Since all curves in figures 2 are parallel to the r axis for $r \lesssim 100$ cm, we conclude that any inhomogeneous model that satisfies the limits on light element abundances will give the same abundances as the homogeneous model, and the same limits on η ($2.8 \lesssim \eta_{10} \lesssim 3.3$, WSSOK). Since the hatched regions cover an almost identical area, this conclusion is independent of R and f_v. We have also verified that in the large r limit (no diffusion) yields become independent of r.

If we relax the upper limit on ^{7}Li, (say, because of some subsequent Li destruction) there is little change unless we also relax the upper limit on ^{4}He. The dashed curve in figures 2 represent a ^{4}He mass fraction of 0.245. In the case where $Y_p < 0.245$ there are two allowed regions if we allow the primordial abundance of ^{7}Li to exceed 4×10^{-10}: (1) the previous limits are now $2.8 \lesssim \eta_{10} \lesssim 6$ and $r \lesssim 100$ cm; (2) there is a region between the ^{2}H+^{3}He curve and the dashed curve at $\eta \sim 7$, $r \sim 10^4$. This solution however requires a rather finely tuned value of r in addition to the excess production of ^{7}Li, which would require the depletion of ^{7}Li by more than factor of 4 (we note that standard stellar models (Deliyannis, Demarque & Kawaler 1990) do not deplete ^{7}Li significantly and non-standard stellar models which do deplete ^{7}Li are highly constrained by the observation of ^{6}Li in HD 84937 (Steigman et al. 1993)). Furthermore, since the code calculates abundances for a uniform lattice of spheres an accurate determination of yields in this case would require an averaging over a distribution of values for r. Given the narrowness of the allowed r values for the second solution it seems highly unlikely that realistic averaging would result in a solution satisfying all the light element abundances (Meyer et al. 1991) notwithstanding the problem with ^{7}Li.

Abundances of ^{6}Li, ^{9}Be, ^{10}B and ^{11}B are shown in figures 3–6. With the exception of ^{9}Be these are maximal abundances for all values of R, f_v. Curves are given for $\eta_{10} = 3.0$, 7.0, and 70.0. Yields of these elements are again independent of r for $r \lesssim 100$ cm, indicating that the yields are unchanged from those of homogeneous nucleosynthesis. For $\eta_{10} = 3$ this gives a ^{6}Li abundance (number density relative to H) of roughly 3×10^{-14}, a factor of 100 lower than the recent measurement of Smith, Lambert, & Nissen (1992). Allowing for a higher ^{4}He abundance and abandoning the ^{7}Li constraints (that is, the $\eta_{10} \sim 7$, $r \sim 10^4$

solution mentioned earlier) increases the yield by (at most) a factor of 10. Of course if we now require the depletion of ^{7}Li, ^{6}Li will be severely depleted (Brown and Schramm 1988) and the discrepancy is amplified.

The ^{9}Be abundance (figure 4) is shown as maximal abundances for R = 100, 1000, $f_v = 1/64$, $1/8$ (solid curve) and as abundances for $R = 10^6$, $f_v = 1/64$ (dashed curve). In this case, the effect of increasing R was greatest. For $r \lesssim 100$ cm, the ^{9}Be abundance is 1×10^{-18}, four orders of magnitude below the observations (Rebolo et al. 1988; Ryan et al. 1992; Gilmore, Edvardsson, & Nissen 1991;). Allowing for $\eta_{10} \sim 5$, $r \sim 10^4$ cm raises this almost to 10^{14} (higher if we accept a density contrast of $R = 10^6$), however we regard this as an extremely unlikely situation. Note that even though ^{9}Be reaches a maximum at a few $\times 10^{-14}$ for $\eta_{10} = 70$, the other light elements are irreconcilably off from their measured abundances, and this case is thus not viable.

^{10}B (figure 5) and ^{11}B (figure 6) have abundances of $\sim 10^{-19}$ and $\sim 10^{-17}$, respectively 7 and 5 orders of magnitude below observations (Duncan, Lambert, & Lemke 1992). (The ^{10}B abundance is always negligible compared to the ^{11}B abundance which is problematic if one wishes to show that the observed B is primordial; the two isotopes are observed with comparable abundances.) Using $\eta_{10} \sim 5$ and $r \sim 10^4$ raises both abundance by less than two orders of magnitude. We emphasize that high abundances of ^{11}B are produced only for large η, and at a value of r where the ^{9}Be abundance is low. Thus it is not possible to reconcile the large r model with the observed B to Be ratio, regardless of the problems with the light elements.

We also show maximum (solid) and minimum (dashed) yields of ^{4}He and ^{7}Li in figures 7 and 8. The possibility of a low ^{4}He abundance in inhomogeneous models was also investigated in Mathews, Schramm, & Meyer (1993).

4. Post-Processing

We implemented the hydrodynamic-Thomson-drag dissipation effect by running the inhomogeneous code to a mixing temperature $T_m = 20$ keV, the favored value given in Alcock et al. (1990). We then homogenized the results and continued to run down to the usual final temperature $T_f = 10^7\mathrm{K} = 1.2$ keV. While the effects of post-processing on the lightest element (D, ^{3}He, ^{7}Li) depend rather strongly on the input parameters, we did find consistent results for Be and B. The result is a reduction in the yield of ^{9}Be and ^{10}B, and an increase in ^{11}B. While it is conceivable that the right set of parameters might bring this model into agreement with the observations of the very light elements, the increase in B combined with a decrease in Be is difficult to reconcile with the observations (Duncan et al., 1992). Consequently, we regard this as an unlikely scenario. Similar conclusions have been reached in the recent parameter-free hydrodynamic calculations of Jedamzik & Fuller (1993).

5. Conclusions

With the accepted limits on the light element abundances (^{4}He, ^{2}H, ^{3}He, ^{7}Li) the length scale of inhomogeneities at the epoch of primordial nucleosynthesis is constrained to be $r \lesssim 100$ cm (at 100 MeV). With this constraint, the abundances of the light elements, and of the additional elements ^{6}Li, ^{9}Be, ^{10}B and ^{11}B are largely indistinguishable from those of homogeneous nucleosynthesis. In particular, the abundances of LiBeB are lower (by several orders of magnitude) than the lowest of the abundances seen recently in population II halo stars. We conclude that these elements must be produced by some process other than primordial nucleosynthesis.

If we push the limits on the light element abundances to the extreme, we find that while the abundances of LiBeB all increase, only ^{9}Be is raised significantly and still falls short of being able to explain any of the recent observations.

Acknowledgements

This work was supported in part by the NSF, by the DOE and by NASA at the University of Chicago, by the DOE and by NASA theory grant 2381 at Fermilab, by DOE grant DE-AC02-83ER-40105 and by a Presidential Young Investigator Award at the University of Minnesota. Work performed in part under the auspices of the U.S. Department of Energy at Lawrence Livermore National Laboratory under contract number W-7405-ENG-48 and Nuclear Theory grant SF-ENG-48.

References

Alcock, C.R., Dearborn, D.S., Fuller, G.M., Mathews, G.J., & Meyer, B.S., 1990, ApJ, 64, 2607

Alcock, C., Fuller, G.M., & Mathews, G.J. 1987, ApJ, 320, 439

Applegate, J.H., & Hogan, C.J. 1985, Phys. Rev., D31, 3037; erratum in D34, 1938

Applegate, J.H., Hogan, C.J., & Scherrer, R. 1987, Phys. Rev., D35, 1151

Campbell, B.A., Ellis, J., & Olive, K.A. 1990, Nucl. Phys. B345, 57

Crawford, M., & Schramm D.N. 1982, Nature, 298, 538

Banerjee, B., & Chitre, S.M. 1991, Phys. Lett., B258, 247

Boyd, R.N., & Kajino, T. 1989, ApJ, 336, L55

Brown, L. & Schramm, D.N. 1988, ApJ, 329,L103

Deliyannis, C. P., Demarque, P., & Kawaler, S. D. 1990 ApJS, 73, 21

Duncan, D.K., Lambert, D.L., & Lemke, M. 1992, ApJ, 401, 584

Fahri, E. & Jaffe, R.L. 1984, Phys. Rev. D30, 2379

Fields, B., Schramm, D.N., & Truran J. 1993, Fermilab preprint 92-114

Fuller, G.M., Mathews G.J., & Alcock, C.R. 1988, Phys. Rev., D37, 1380

Fowler, W.A., & Hoyle, F. 1964, ApJS, 9, 201

Gilmore, G., Edvardsson, B., & Nissen, P.E. 1991, ApJ, 378, 17

Gnedin, N.Yu., & Ostriker, J.P., 1992, ApJ, 400, 1

Heckler A. & Hogan, C.J. 1993, Phys. Rev. D, submitted

Hobbs, L.M., & Duncan, D.K. 1987, ApJ, 317, 796

Hogan, C. 1983, Phys. Lett., B133,172

Iso, K., Kodama, H., & Sato, K. 1986, Phys. Lett., B169, 337

Jedamzik, K., Fuller, G.M., & Mathews, G.J. 1993a, ApJ, submitted

Jedamzik, K., Fuller, G.M., Mathews, G.J., & Kajino, T. 1993b, ApJ, in press

Jedamzik, K., & Fuller, G.M., 1993, ApJ, in press.

Kajantie, K., Karkkainen, L., & Rummukainen, K., 1990, Nucl. Phys., B333, 100.

Kapusta, J., & Olive, K.A. 1988, Phys. Lett., B209, 295

Kurki-Suonio, H. 1988, Phys. Rev., D37, 2104

Kurki-Suonio, H., Aufderheide, M.B., Graziani, F., Mathews, G.J., Banerjee, B., Chitre, S.M., & Schramm, D.N. 1992, Phys. Lett. B, 289, 211

Kurki-Suonio, H., & Matzner, R.A. 1989, Phys. Rev. D, 39, 1046

Kurki-Suonio, H., & Matzner, R.A. 1990, Phys. Rev. D, 42, 1047

Kurki-Suonio, H., Matzner, R.A., Olive, K.A., & Schramm, D.N. 1990, ApJ, 353,406

Malaney, R.A., & Fowler, W.A. 1988, ApJ, 333, 14

Malaney, R.A., & Fowler, W.A. 1989, ApJ, 345, L5

Malaney, R.A., & Mathews, G.J. 1993, Phys. Rep. (in press)

Mathews, G.J., Meyer, B.S., Alcock, C.R., & Fuller, G.M. 1990, ApJ, 358, 36

Mathews, G.J., Schramm, D.N., & Meyer, B.S., 1993, ApJ, 404, 476

Meyer, B.S., Alcock, C.R., Mathews, G.J., & Fuller, G.M. 1991, Phys. Rev. D43, 1079

Olive, K. A., & Schramm, D. N. 1992 Nature, 360,439

Particle Data Group, 1992, Phys. Rev. D45.

Prantzos, N., Cassé, M., & Vangioni-Flam, E. 1993 ApJ, 403, 630

Rebolo, R., Molaro, P., Abia, C., & Beckman, J.E. 1988, A&A, 193, 193

Rebolo, R., Molaro, P., & Beckman, J.E. 1988, A&A, 192, 192

Ryan, S.G., Norris, J.E., Bessell, M.S., & Deliyannis, C.P. 1992, ApJ, 388, 184

Sale, K.E., Mathews, G.J. 1986, ApJ Lett., 309, L1

Skillman, E. et al. 1993, in *Texas/PASCOS 92: Relativistic Astrophysics and Particle Cosmology* eds. C.W. Akerlof & M.A. Srednicki, (New York Academy of Sciences, New York) p.739

Smith, V.V., Lambert, D.L., & Nissen, P.E. 1992, University of Texas preprint

Spite, F., & Spite, M. 1982a Nature, 297, 483

Spite, F., & Spite, M. 1982b A&A, 115, 357

Spite, F., & Spite, M. 1986 A&A, 163, 140

Steigman, G., Fields, B., Olive, K.A., Schramm, D.N., & Walker, T. 1993, University of Minnesota preprint UMN-TH-1123/93

Steigman, G., & Walker, T.P. 1992, ApJ, 385, L13

Terasawa, N., & Sato, K. 1989a, Phys. Rev., D39, 2893

Terasawa, N., & Sato, K. 1989b, Prog. Theor. Phys., 81, 254

Terasawa, N., & Sato, K. 1989c, Prog. Theor. Phys., 81, 1085

Thomas, D., Schramm, D.N., Olive, K.A., & Fields, B.D. 1993, ApJ, 406, 569 (TSOF)

Wagoner, R.V. 1973, ApJ, 179,343

Walker, T.P., Steigman, G., Schramm, D.N., Olive, K.A., & Fields, B. 1993, preprint (Fermilab-Pub-92/199-A) ApJ (in press)

Walker, T.P., Steigman, G., Schramm, D.N., Olive, K.A., & Kang, H.-S. 1991, ApJ, 376, 51

Witten, E. 1984, Phys. Rev., D30, 272

Yang, J., Turner, M.S., Steigman, G., Schramm, D.N., & Olive, K.A. 1984, ApJ, 281,493

Table 1
Reactions changed since TSOF

Reaction	Rate
$^{12}Be(\beta^-)^{12}B$	34.31 ± 0.03
$^{13}B(\beta^-)^{13}C$	40.00 ± 0.40
$^{14}B(\beta^-)^{14}C$	43.05 ± 3.21
$^{8}He(\beta^-)^{8}Li$	5.68 ± 0.09
$^{11}Li(\beta^-)^{11}Be$	79.7 ± 0.9
$^{15}B(\beta^-)^{15}C$	63 ± 6
$^{17}C(\beta^-)^{17}N$	3.43 ± 0.29
$^{18}C(\beta^-)^{18}N$	$10.5^{+2.4}_{-4.0}$
$^{18}N(\beta^-)^{18}O$	1.10 ± 0.06
$^{19}C(\beta^-)^{19}N$	57.8
$^{19}N(\beta^-)^{19}O$	3.3 ± 1.7
$^{20}C(\beta^-)^{20}N$	74.5
$^{20}N(\beta^-)^{20}O$	$6.9^{+1.4}_{-2.1}$
$^{21}O(\beta^-)^{21}F$	0.202 ± 0.006
$^{22}O(\beta^-)^{22}F$	0.308 ± 0.67
$^{22}F(\beta^-)^{22}Ne$	0.1639 ± 0.0015
$^{23}F(\beta^-)^{23}Ne$	0.31 ± 0.06
$^{24}F(\beta^-)^{24}Ne$	2.04 ± 0.48
$^{18}O(n,\gamma)^{19}O$	$21 \pm 1 + 7.3 \times 10^5\, T_9^{-3/2} \exp(-1.846/T_9) + 1.3 \times 10^5$
$^{11}B(n,\gamma)^{12}B$	$1.3 \times 10^5\, T_9^{-3/2} \exp(-0.2112/T_9) + 4.0 \times 10^5\, T_9^{-3/2} \exp(-4.53/T_9)$ $+1.3 \times 10^5$
$^{12}B(n,\gamma)^{13}B$	$1.3 \times 10^6\, T_9^{-3/2} \exp(-1.64/T_9) + 1.3 \times 10^5$
$^{13}B(n,\gamma)^{14}B$	$2.8 \times 10^4\, T_9^{-3/2} \exp(-4.02/T_9) + 1.3 \times 10^5$
$^{19}O(n,\gamma)^{20}O$	$4.6 \times 10^6\, T_9^{-3/2} \exp(-0.186/T_9) + 4.6 \times 10^6\, T_9^{-3/2} \exp(-1.74/T_9)$ $+1.3 \times 10^5$
$^{21}F(n,\gamma)^{22}F$	$1.8 \times 10^6\, T_9^{-3/2} \exp(-4.18/T_9) + 1.3 \times 10^5$
$^{11}Be(n,\gamma)^{12}Be$	1.3×10^5
$^{14}B(n,\gamma)^{15}B$	1.3×10^5
$^{16}C(n,\gamma)^{17}C$	1.3×10^5
$^{17}C(n,\gamma)^{18}C$	1.3×10^5
$^{18}C(n,\gamma)^{19}C$	1.3×10^5
$^{19}C(n,\gamma)^{20}C$	1.3×10^5
$^{17}N(n,\gamma)^{18}N$	1.3×10^5
$^{18}N(n,\gamma)^{19}N$	1.3×10^5
$^{19}N(n,\gamma)^{20}N$	1.3×10^5
$^{20}O(n,\gamma)^{21}O$	1.3×10^5
$^{21}O(n,\gamma)^{22}O$	1.3×10^5
$^{8}He(p,n)^{8}Li$	$0.2874 \times 10^{11}\, T_9^{-2/3} \exp(-6.4847/T_9^{1/3})$
$^{8}He(p,\gamma)^{9}Li$	ditto

Table 1 (contd.)

Reaction	Rate
^{11}Li(p,n)^{11}Be	$0.1149 \times 10^{12}\, T_9^{-2/3} \exp(-8.5850/T_9^{1/3})$
^{11}Li(p,α)^{8}He	ditto
^{11}Li(p,γ)^{12}Be	ditto
^{12}Be(p,n)^{12}B	$0.3247 \times 10^{12}\, T_9^{-2/3} \exp(-10.4242/T_9^{1/3})$
^{12}Be(p,α)^{9}Li	ditto
^{12}Be(p,γ)^{13}B	ditto
^{13}B(p,n)^{13}C	$0.7917 \times 10^{12}\, T_9^{-2/3} \exp(-12.1202/T_9^{1/3})$
^{13}B(p,α)^{10}Be	ditto
^{13}B(p,γ)^{14}C	ditto
^{14}B(p,n)^{14}C	$0.8355 \times 10^{12}\, T_9^{-2/3} \exp(-12.1408/T_9^{1/3})$
^{14}B(p,α)^{11}Be	ditto
^{14}B(p,γ)^{15}C	ditto
^{15}B(p,n)^{15}C	$0.8788 \times 10^{12}\, T_9^{-2/3} \exp(-12.15887/T_9^{1/3})$
^{15}B(p,α)^{12}Be	ditto
^{15}B(p,γ)^{16}C	ditto
^{15}C(p,n)^{15}N	$0.1850 \times 10^{13}\, T_9^{-2/3} \exp(-13.73032/T_9^{1/3})$
^{15}C(p,α)^{12}B	ditto
^{15}C(p,γ)^{16}N	ditto
^{16}C(p,n)^{16}N	$0.1950 \times 10^{13}\, T_9^{-2/3} \exp(-13.74825/T_9^{1/3})$
^{16}C(p,α)^{13}B	ditto
^{16}C(p,γ)^{17}N	ditto
^{17}C(p,n)^{17}N	$0.2049 \times 10^{13}\, T_9^{-2/3} \exp(-13.76414/T_9^{1/3})$
^{17}C(p,α)^{14}B	ditto
^{17}C(p,γ)^{18}N	ditto
^{18}C(p,n)^{18}N	$0.2147 \times 10^{13}\, T_9^{-2/3} \exp(-13.77833/T_9^{1/3})$
^{18}C(p,α)^{15}B	ditto
^{18}C(p,γ)^{19}N	ditto
^{19}C(p,n)^{19}N	$0.2246 \times 10^{13}\, T_9^{-2/3} \exp(-13.79108/T_9^{1/3})$
^{19}C(p,γ)^{20}N	ditto
^{20}C(p,n)^{20}N	$0.2343 \times 10^{13}\, T_9^{-2/3} \exp(-13.80259/T_9^{1/3})$
^{20}C(p,γ)^{21}N	ditto
^{17}N(p,n)^{17}O	$0.4024 \times 10^{13}\, T_9^{-2/3} \exp(-15.25388/T_9^{1/3})$
^{17}N(p,α)^{14}C	ditto
^{17}N(p,γ)^{18}O	ditto
^{18}N(p,n)^{18}O	$0.4235 \times 10^{13}\, T_9^{-2/3} \exp(-15.26960/T_9^{1/3})$
^{18}N(p,α)^{15}C	ditto
^{18}N(p,γ)^{19}O	ditto
^{19}N(p,n)^{19}O	$0.4445 \times 10^{13}\, T_9^{-2/3} \exp(-15.28373/T_9^{1/3})$
^{19}N(p,γ)^{20}O	ditto

Table 1 (contd.)

Reaction	Rate
^{19}N(α,p)^{22}O	$0.5537 \times 10^{18}\, T_9^{-2/3} \exp(-36.75954/T_9^{1/3})$
^{20}N(p,n)^{20}O	$0.4656 \times 10^{13}\, T_9^{-2/3} \exp(-15.29649/T_9^{1/3})$
^{20}N(p,α)^{17}C	ditto
^{20}N(p,γ)^{21}O	ditto
^{20}O(p,n)^{20}F	$0.8705 \times 10^{13}\, T_9^{-2/3} \exp(-16.72064/T_9^{1/3})$
^{20}O(p,γ)^{21}F	ditto
^{21}O(p,n)^{21}F	$0.9127 \times 10^{13}\, T_9^{-2/3} \exp(-16.73330/T_9^{1/3})$
^{21}O(p,γ)^{22}F	ditto
^{22}O(p,n)^{22}F	$0.9552 \times 10^{13}\, T_9^{-2/3} \exp(-16.74484/T_9^{1/3})$
^{22}F(p,α)^{19}O	$0.1712 \times 10^{14}\, T_9^{-2/3} \exp(-18.11268/T_9^{1/3})$
^{11}B(α,γ)^{15}N	$0.4314 \times 10^{16}\, T_9^{-2/3} \exp(-28.22994/T_9^{1/3})$
^{9}Li(α,n)^{12}B	$0.6221 \times 10^{14}\, T_9^{-2/3} \exp(-19.70047/T_9^{1/3})$
^{10}B(α,γ)^{14}N	$0.3251 \times 10^{16}\, T_9^{-2/3} \exp(-27.98338/T_9^{1/3})$
^{8}B(α,γ)^{12}N	$0.1662 \times 10^{16}\, T_9^{-2/3} \exp(-27.34717/T_9^{1/3})$
^{17}N(α,p)^{20}O	$0.3805 \times 10^{18}\, T_9^{-2/3} \exp(-36.51220/T_9^{1/3})$
^{16}C(α,γ)^{20}O	$0.6796 \times 10^{17}\, T_9^{-2/3} \exp(-32.81660/T_9^{1/3})$

Figure Captions

1 The nuclear reaction network used in all calculations.

2a Limits on r and η due to the light element abundances, for $R = 100$. Curves show the most generous limits for $f_v = 1/8$ and $f_v = 1/64$, and represent the following abundances: ^{2}H/H $= 1.8 \times 10^{-5}$, (^{2}H+^{3}He)/H $= 1.0 \times 10^{-4}$, ^{7}Li/H $= 1.4 \times 10^{-10}$, $Y_p = 0.22, 0.24$. The dashed curve is for $Y_p = 0.245$. The hatched area shows the region allowed by the light element abundances.

2b As figure 2, for $R = 1000$.

2c As figure 2, but for $R = 10^6$, $f_v = 1/64$.

3 ^{6}Li abundance as a function of r for $\eta_{10} = 3, 7, 70$ ($\eta_{10} = 70$ is included only for illustrative purposes, as the light element abundances can never all be fit in this case). The curves represent the most generous abundances for all values of R, f_v. The hatched line shows the upper limit on r.

4 As figure 3, with ^{9}Be abundances, except that the solid curves represent the maximum yields for all of $R = 100, 1000$, $f_v = 1/8, 1/64$ and the dashed curves represent yields for $R = 10^6$, $f_v = 1/64$.

5 As figure 3, with ^{10}B abundances.

6 As figure 3, with ^{11}B abundances.

7 As figure 3, with ^{4}He abundances. In addition, the dashed line shows the lowest yield for all R, f_v.

8 As figure 7, with ^{7}Li abundances.

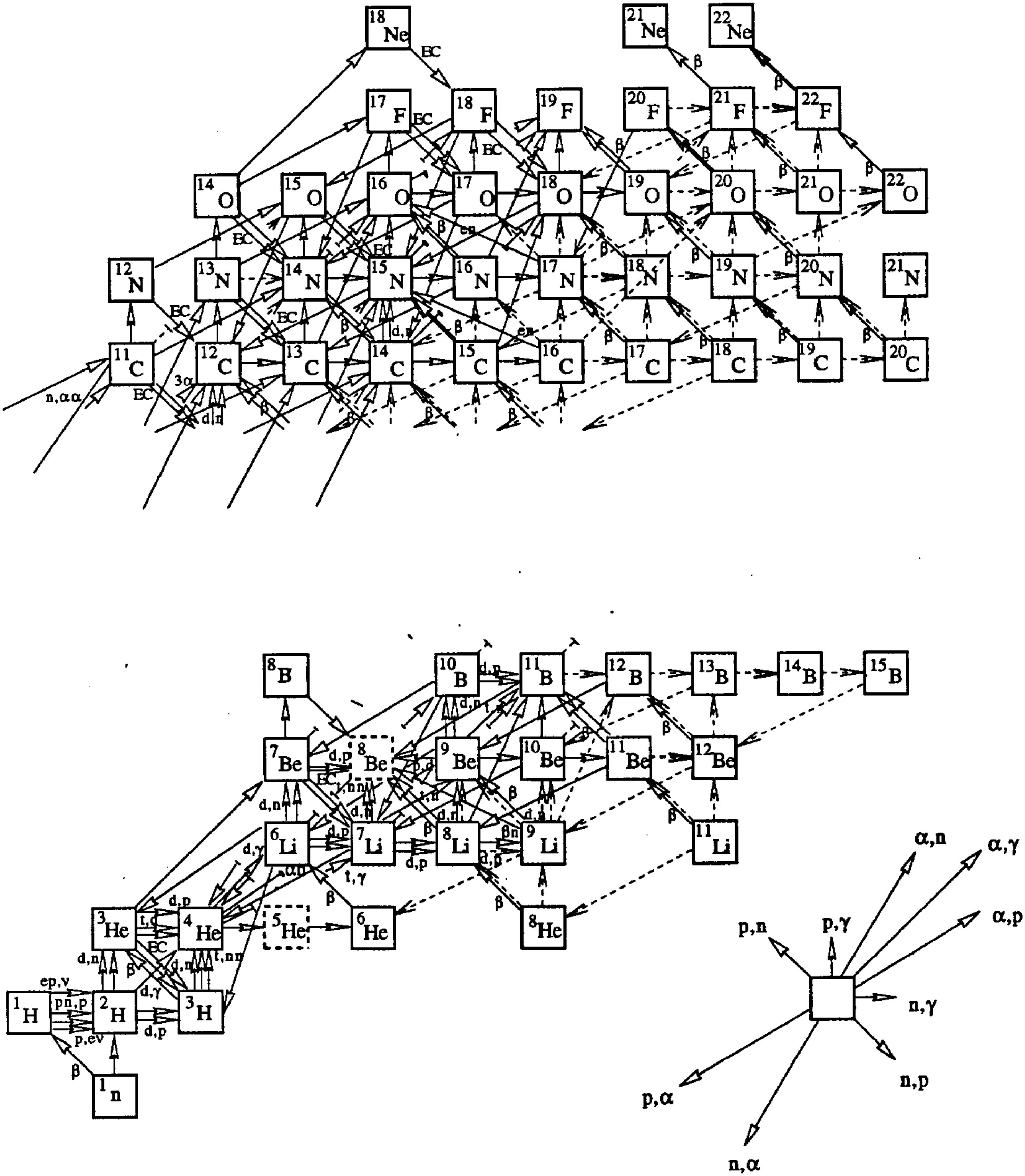

18Ne
21Ne
22Ne
17F
18F
19F
20F
21F
22F
14O
15O
16O
17O
18O
19O
20O
21O
22O
12N
13N
14N
15N
16N
17N
18N
19N
20N
21N
11C
12C
13C
14C
15C
16C
17C
18C
19C
20C
n,αα
3α
EC
β
8B
10B
11B
12B
13B
14B
15B
7Be
8Be
9Be
10Be
11Be
12Be
6Li
7Li
8Li
9Li
11Li
3He
4He
5He
6He
8He
1H
2H
3H
1n
ep,ν
pn,p
p,eν
d,n
d,p
d,γ
t,γ
βn
α,n
α,γ
α,p
p,n
p,γ
n,γ
n,p
p,α
n,α

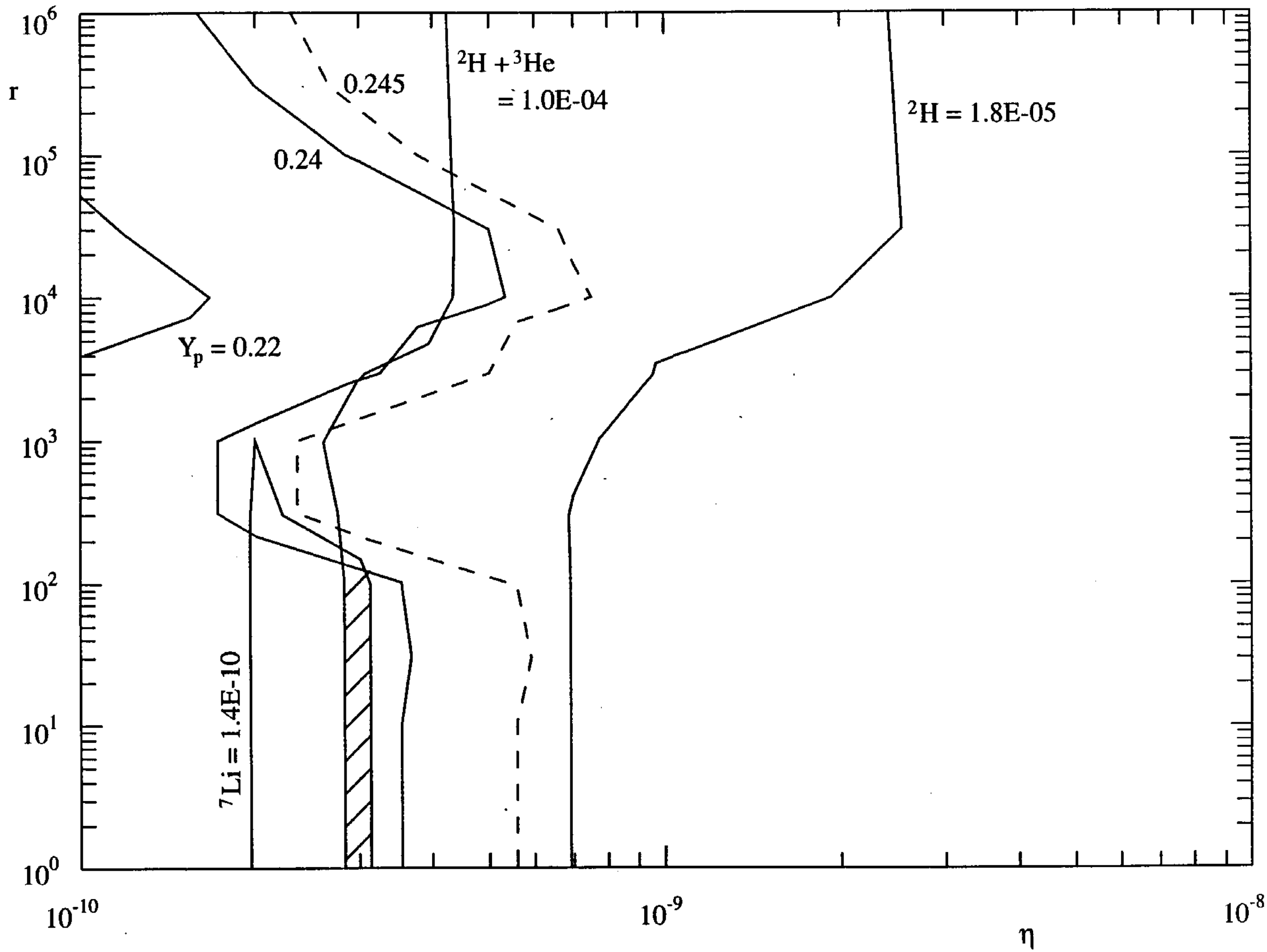

r
η
10^{6}
10^{5}
10^{4}
10^{3}
10^{2}
10^{1}
10^{0}
10^{-10}
10^{-9}
10^{-8}
$^{2}H + ^{3}He$
$= 1.0E-04$
$^{2}H = 1.8E-05$
0.245
0.24
$Y_p = 0.22$
$^{7}Li = 1.4E-10$

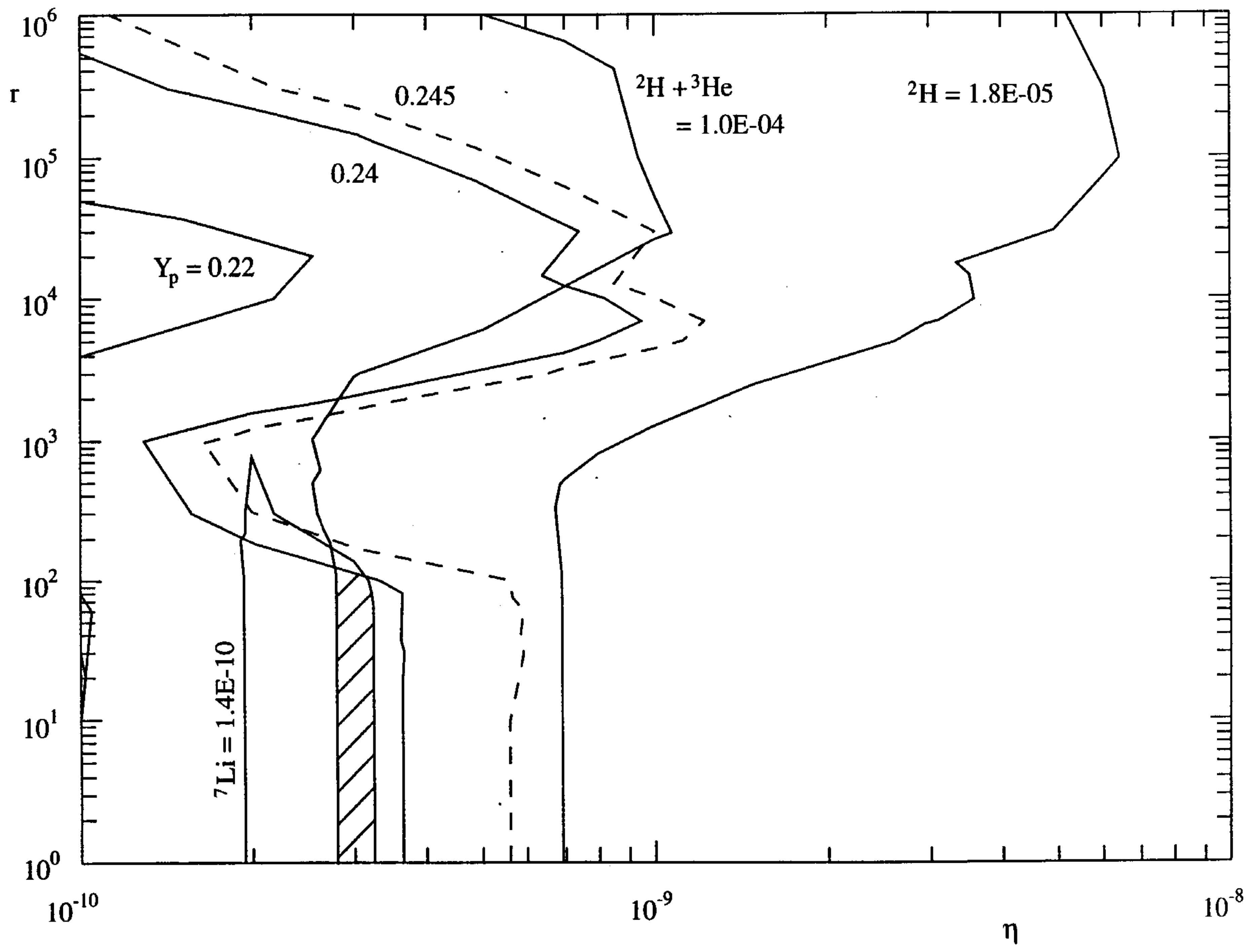
r
η
10^6
10^5
10^4
10^3
10^2
10^1
10^0
10^{-10}
10^{-9}
10^{-8}
0.245
0.24
$Y_p = 0.22$
$^2H + ^3He$
$= 1.0E-04$
$^2H = 1.8E-05$
$^7Li = 1.4E-10$

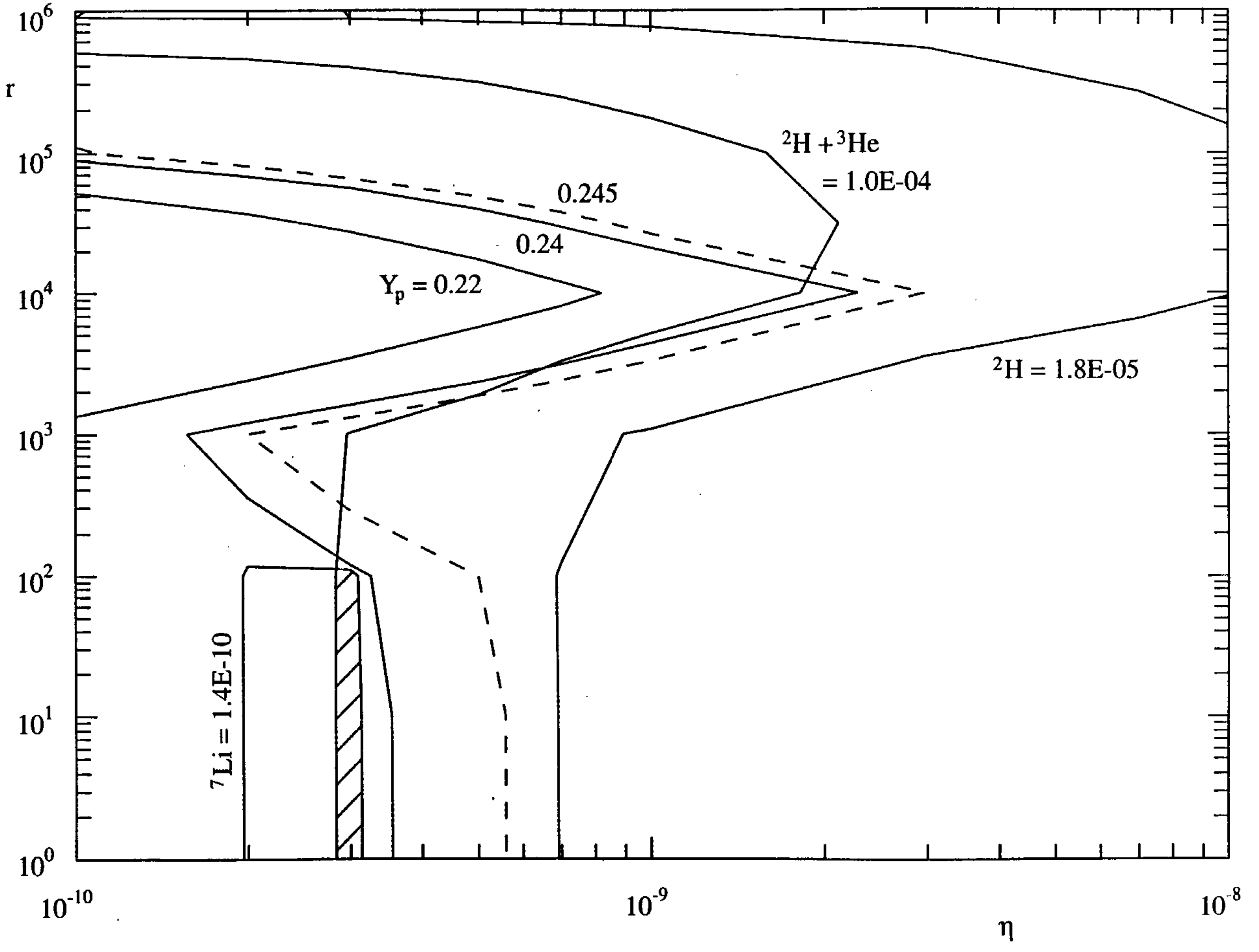

r
10^6
10^5
10^4
10^3
10^2
10^1
10^0
10^{-10}
10^{-9}
10^{-8}
η
$^2H + ^3He$
$= 1.0E-04$
0.245
0.24
$Y_p = 0.22$
$^2H = 1.8E-05$
$^7Li = 1.4E-10$

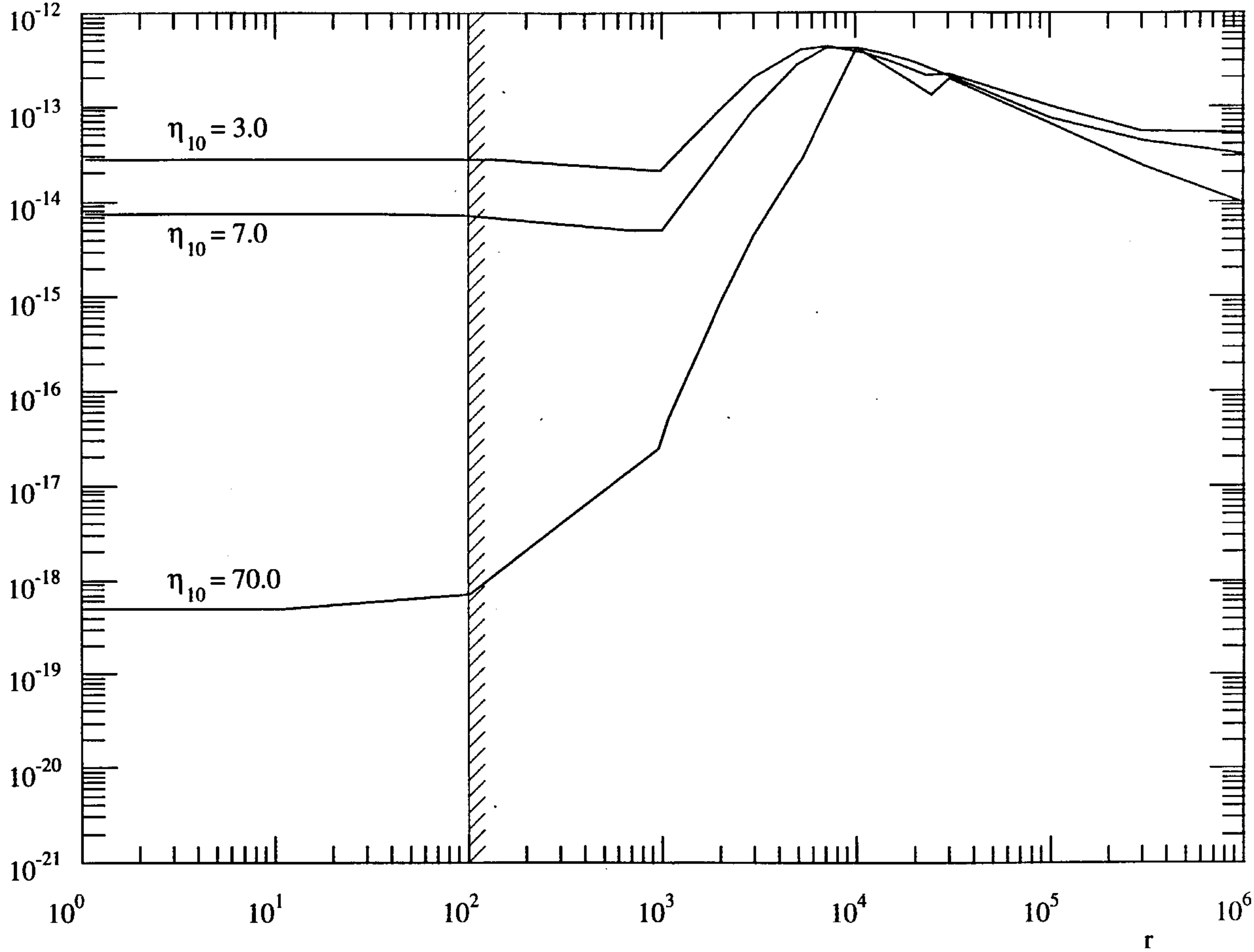

$\eta_{10} = 3.0$
$\eta_{10} = 7.0$
$\eta_{10} = 70.0$
10^{-12}
10^{-13}
10^{-14}
10^{-15}
10^{-16}
10^{-17}
10^{-18}
10^{-19}
10^{-20}
10^{-21}
10^{0}
10^{1}
10^{2}
10^{3}
10^{4}
10^{5}
10^{6}
r

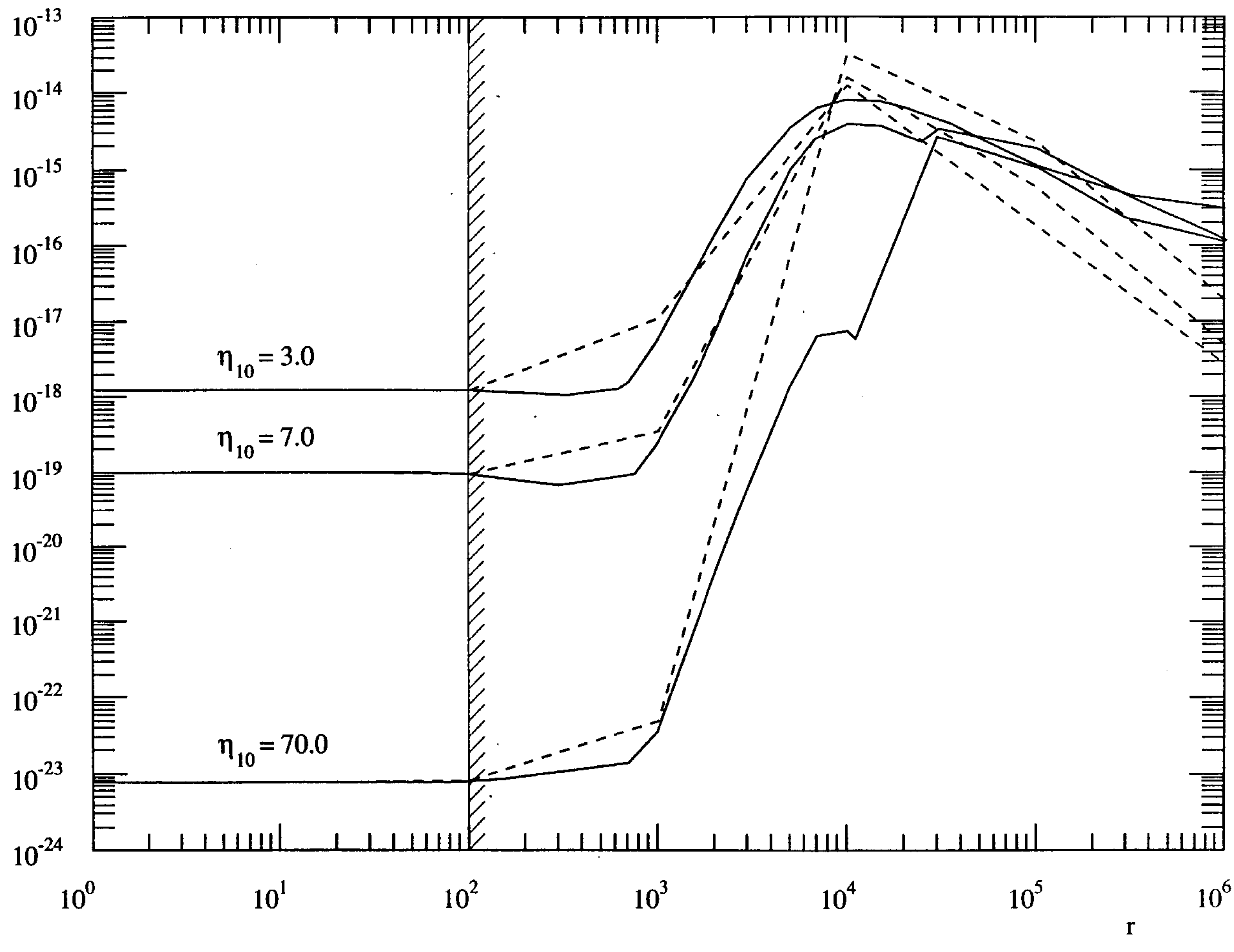

10^{-13}
10^{-14}
10^{-15}
10^{-16}
10^{-17}
10^{-18}
10^{-19}
10^{-20}
10^{-21}
10^{-22}
10^{-23}
10^{-24}
$\eta_{10} = 3.0$
$\eta_{10} = 7.0$
$\eta_{10} = 70.0$
10^{0}
10^{1}
10^{2}
10^{3}
10^{4}
10^{5}
10^{6}
r

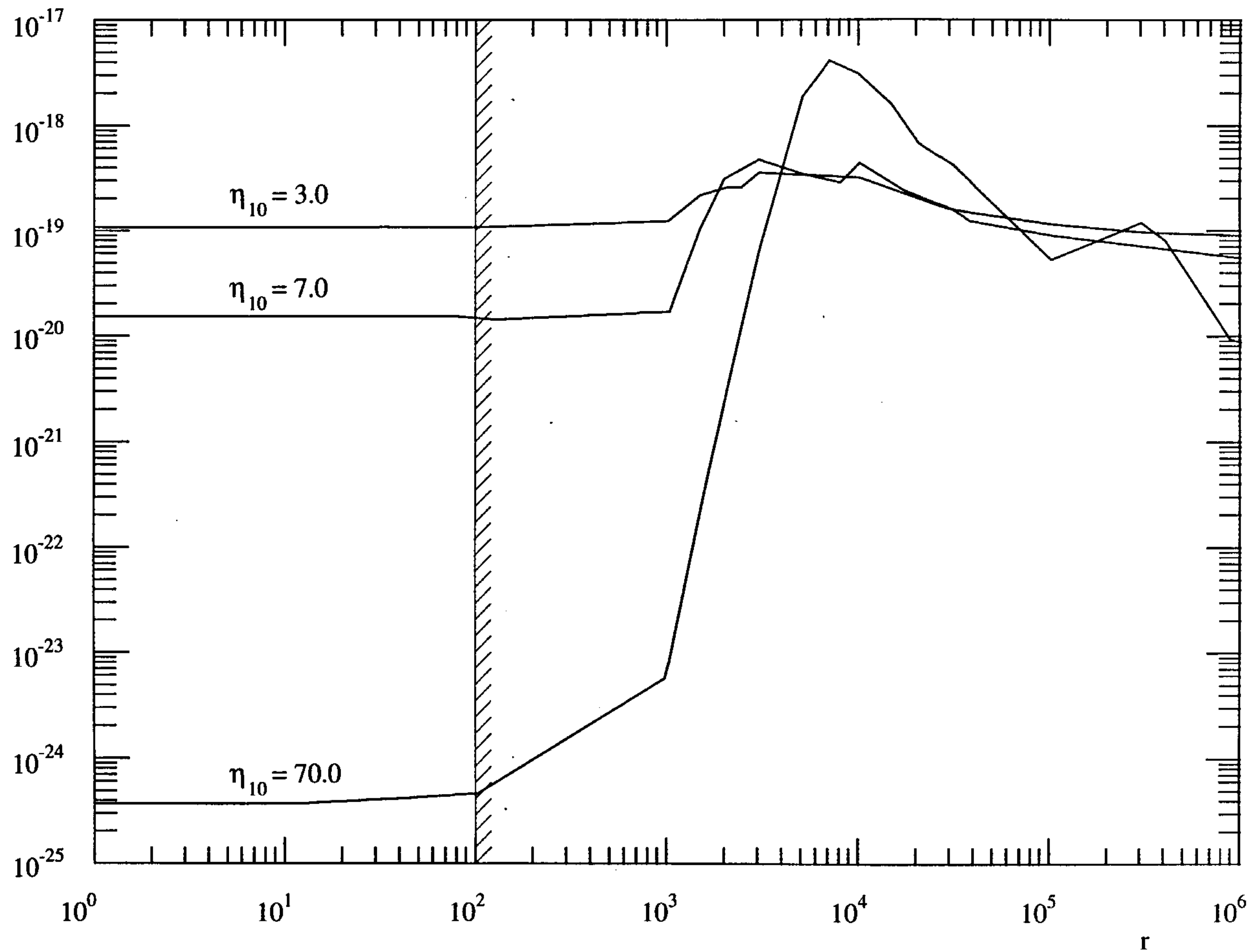
10^{-17}
10^{-18}
10^{-19}
10^{-20}
10^{-21}
10^{-22}
10^{-23}
10^{-24}
10^{-25}
$\eta_{10} = 3.0$
$\eta_{10} = 7.0$
$\eta_{10} = 70.0$
10^0
10^1
10^2
10^3
10^4
10^5
10^6
r

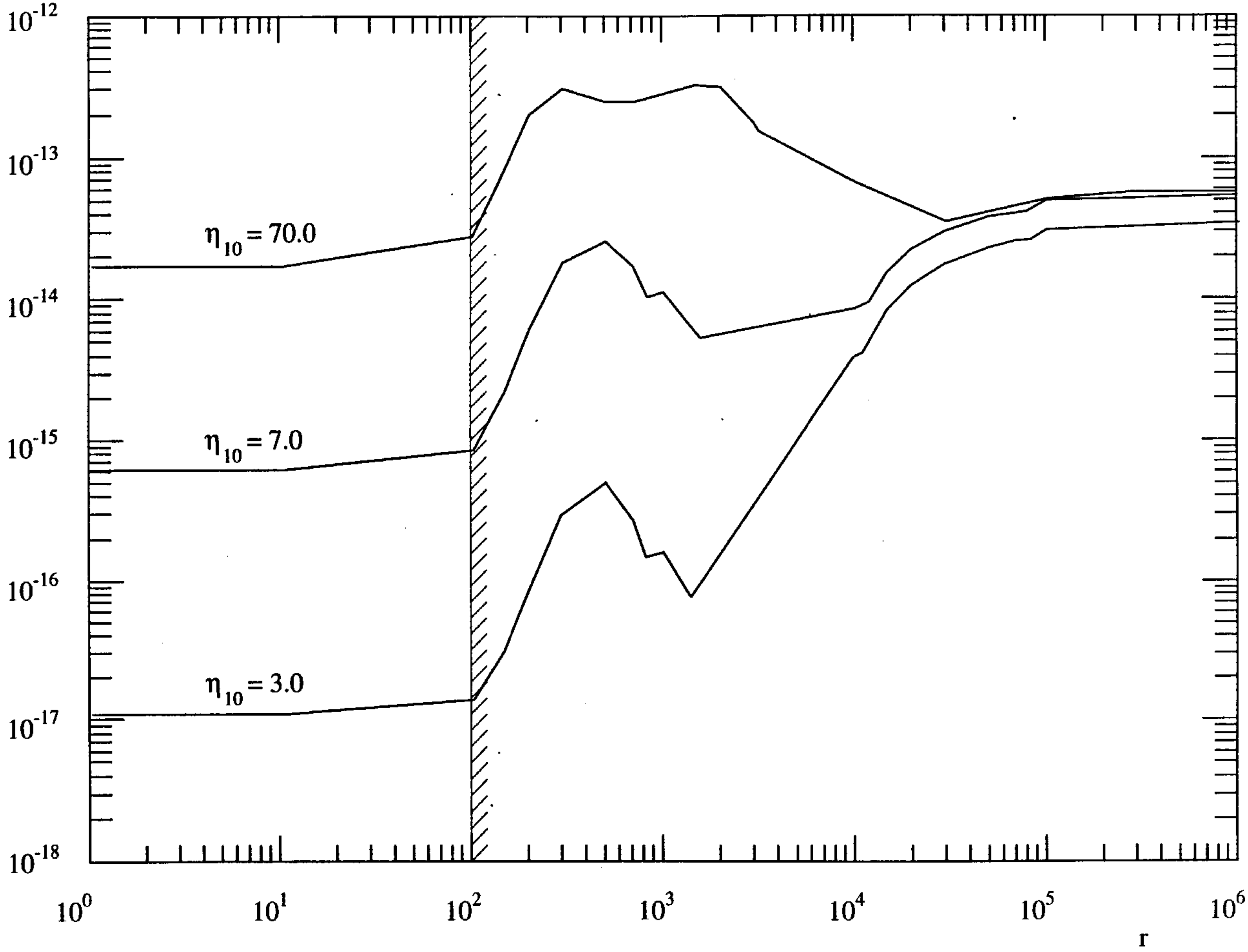

10^{-12}
10^{-13}
10^{-14}
10^{-15}
10^{-16}
10^{-17}
10^{-18}
$\eta_{10} = 70.0$
$\eta_{10} = 7.0$
$\eta_{10} = 3.0$
10^{0}
10^{1}
10^{2}
10^{3}
10^{4}
10^{5}
10^{6}
r

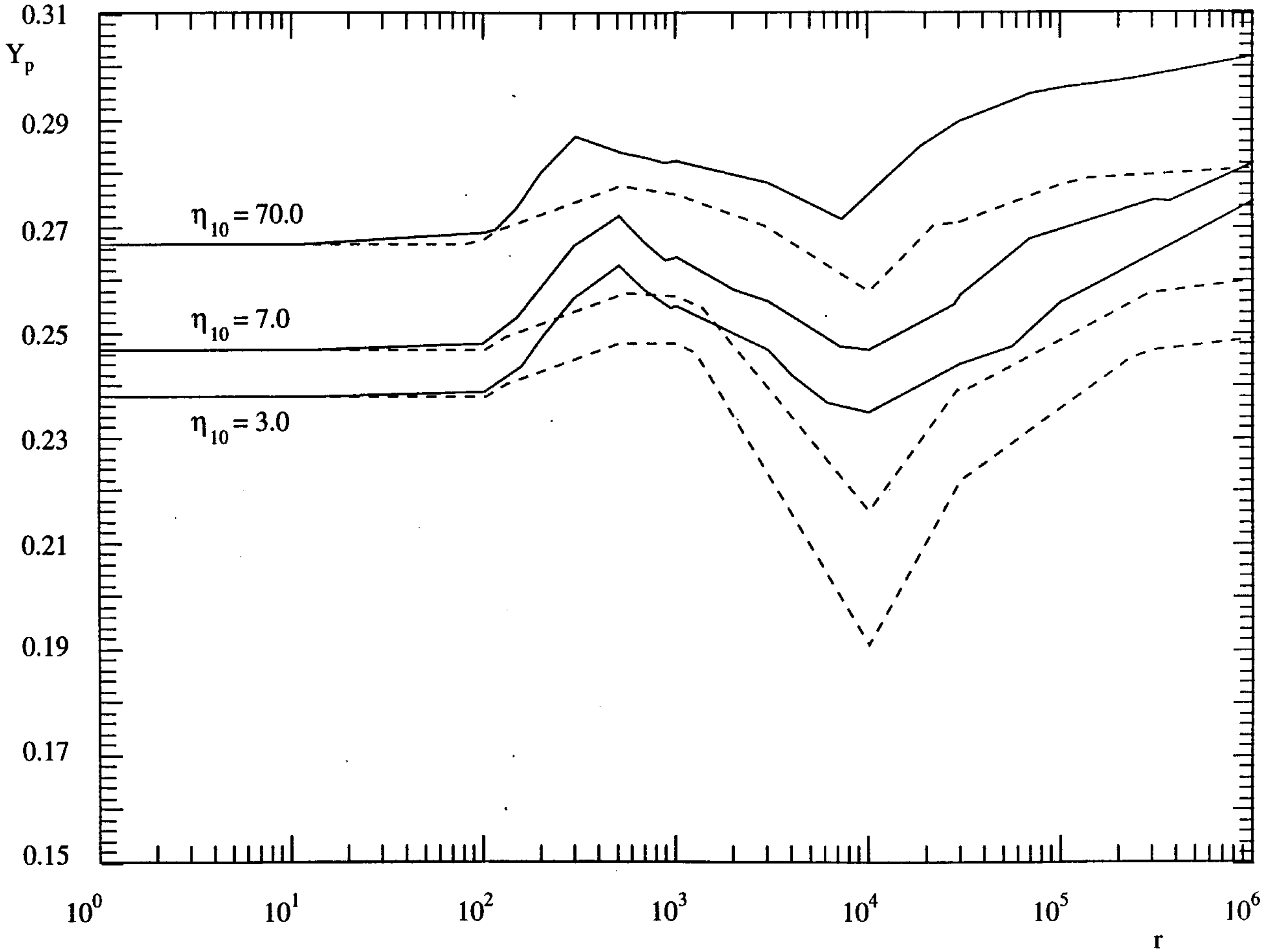

Y_p
0.31
0.29
0.27
0.25
0.23
0.21
0.19
0.17
0.15
$\eta_{10} = 70.0$
$\eta_{10} = 7.0$
$\eta_{10} = 3.0$
10^0
10^1
10^2
10^3
10^4
10^5
10^6
r

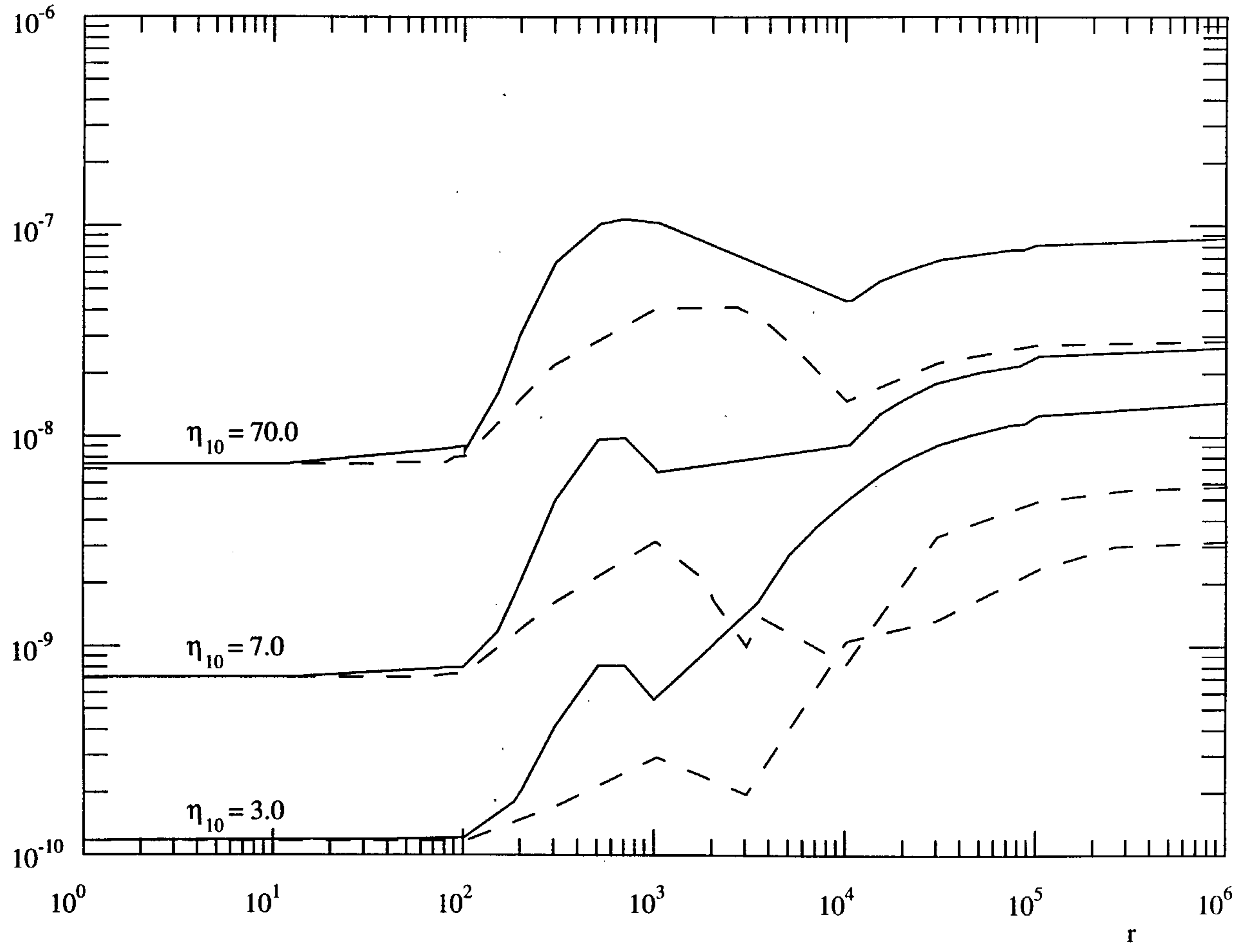

10^-6
10^-7
10^-8
10^-9
10^-10
η10 = 70.0
η10 = 7.0
η10 = 3.0
10^0
10^1
10^2
10^3
10^4
10^5
10^6
r